Growth of Submicrometer-Scale Rectangular Parallelepiped Rutile TiO₂ Films in Aqueous TiCl₃ Solutions under Hydrothermal Conditions

Eiji Hosono, Shinobu Fujihara,* Keita Kakiuchi, and Hiroaki Imai

Department of Applied Chemistry, Faculty of Science and Technology, Keio University, Yokohama 223-8522, Japan

Received March 2, 2004; E-mail: shinobu@applc.keio.ac.jp

Titanium dioxide (TiO₂) exists mainly in three crystal phases: anatase, rutile, and brookite. In contrast to the anatase phase, rutile TiO₂ has attracted less attention in producing catalysts,[1,2] photocatalysts,[3] and dye-sensitized solar cells (DSCs).[4,5] This is attributed to the expectation that the rutile phase may exhibit lower electrochemical performance than the anatase phase, primarily due to differences in their electronic structure. Rutile TiO₂, however, has some advantages over anatase such as higher chemical stability, higher refractive index, cheaper production cost, etc.[5] Furthermore, rutile TiO₂ has been proven to be comparable to anatase in application to DSCs.[4]

The chemical routes to prepare rutile TiO₂ can be classified into three groups.[3] One is the hydrolyzation of titanium alkoxides by sol–gel methods.[6,7] Generally, the rutile phase is obtained by calcination of first crystallized anatase at temperatures higher than 500 °C. Direct formation of rutile at room temperature is also possible through long-term aging of sols or exposure to high relative humidity. The second route is the direct hydrolysis of inorganic salts such as titanium tetrachloride (TiCl₄) in aqueous solutions under hydrothermal or moderate conditions.[8–10] Rutile TiO₂ can be obtained in the form of fine powders. The third method utilizes heterogeneous nucleation in supersaturated aqueous Ti(IV) solutions and is employed to prepare rutile TiO₂ films.[5,11,12] It has been reported that homogeneous rutile films consisting of highly oriented needlelike crystals can be successfully prepared by controlling the reaction rate.[12]

We report here evolution of a new morphology of films consisting of highly crystalline (nearly single-crystalline) rectangular parallelepiped rutile TiO₂ in a submicrometer scale. The films were synthesized via hydrothermal treatments of aqueous titanium trichloride (TiCl₃; 0.15 M) solutions containing a large amount of NaCl (10.0 M). The solutions were placed in Teflon-lined autoclaves. Borosilicate glass slides were used as substrates and immersed in the solutions. The solutions were then heated at 200 °C for typically 3 h. The films deposited on the substrates were rinsed with deionized water and dried at room temperature. Figure 1a is a typical field-emission scanning electron microscope (FE-SEM) image of the film in the middle of the deposition procedure (for 1.5 h). It seems that nucleation of a solid phase initially occurred on some spots of the substrate surface and subsequent crystal growth proceeded radially in the direction of the bulk solution. Panels b and c of Figure 1 are top-images of the film at low and high magnifications, respectively, after deposition for 3 h. The top surface of grains appears to be a gathering of square crystals, while the side surface is relatively smooth. A cross-sectional image shown in Figure 1d indicates that the substrate is covered totally and continuously with the film consisting of rectangular parallelepipeds 150–250 nm in width and 3–4 μm in length (see also Supporting Information). According to an analysis of pore size distribution by nitrogen adsorption–desorption iso-
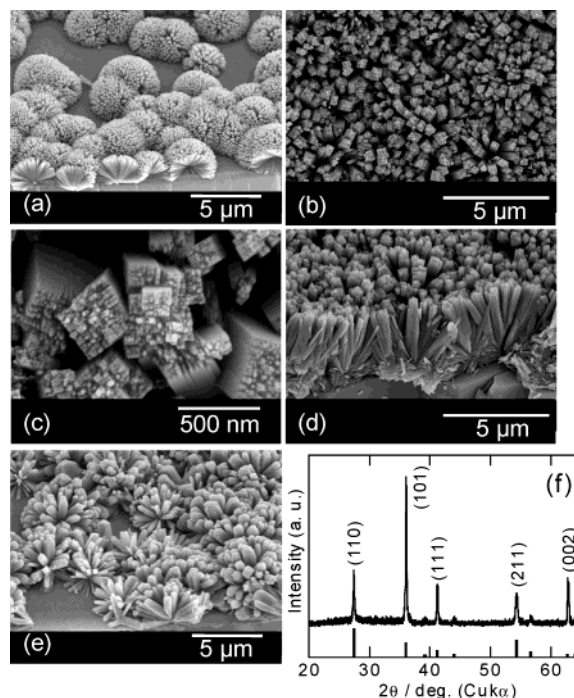
Figure 1. (a) FE-SEM top-image of the film deposited for 1.5 h. (b, c) Top-images of the film deposited for 3 h at low and high magnifications. (d) Cross-sectional view of the film deposited for 3 h. (e) Top-image of the film deposited for 3 h in the solution without addition of NaCl. (f) XRD pattern of the film deposited for 3 h. Vertical bars indicate peak position and intensity of rutile TiO₂ (JCPDS No. 21-1276).

therms, the film had no mesopores (2.0–50 nm) or macropores (at least in the range of 50–100 nm).

For comparison, the solution without addition of NaCl was tested. Figure 1e shows an FE-SEM image of the film after deposition for 3 h. It can be clearly seen that the film growth is relatively retarded as compared to that indicated by the image in b and d. Instead, TiO₂ powders were precipitated in the solution as a result of homogeneous nucleation. Addition of NaCl is therefore a key to achieving the new morphology.

As confirmed by X-ray diffraction (XRD), the films deposited were identified with the rutile TiO₂ phase. Figure 1f shows an XRD pattern (θ–2θ scan) of the film after deposition for 3 h. All the diffraction peaks agree with those of TiO₂ in the rutile form (JCPDS No. 21-1276). Remarkably enhanced (101) and (002) peaks indicate that the film is oriented against the substrate surface. A careful look at the image in Figure 1d reveals that some of the rutile parallelepiped crystals are perpendicular to the substrate surface and some lean toward the azimuthal direction. Because a contact angle between the (101) and the (002) plane is approximately 33°, the orientation observed in the XRD pattern reflects the growth direction of the parallelepiped crystals.
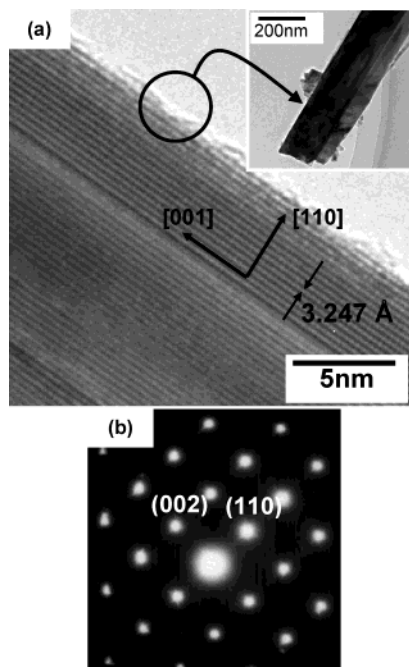
Figure 2. (a) HR-TEM image of one of the rutile TiO₂ rectangular parallelepipeds grown on the substrate. Inset is a low-magnification image. (b) ED pattern of the TiO₂ parallelepiped.

Figure 2a shows a high-resolution transmission electron microscope (HR-TEM) image of the parallelepiped crystal. The surface observed in the image corresponds to the side wall as indicated in an image at a low magnification (an inset of Figure 2a). Lattice images, which are parallel to the wall, can be clearly seen due to phase contrast. The distance between the adjacent lattice fringes can be assigned to the interplaner distance of rutile TiO₂ (110), which is $d_{110} = 3.247$ Å. The [110]-axis is then perpendicular to the wall. The parallelepiped crystals have therefore grown along the [001]-axis that is perpendicular to the [110]-axis. These findings explain the above-mentioned orientation of the films. That is, the enhanced (002) peak results from the crystals that are perpendicular to the substrate surface, while the (101) peak is due to the 33°-inclined crystals.

Figure 2b shows an electron diffraction (ED) pattern of the parallelepiped crystal. A spot pattern indicates a single-crystalline nature of the rutile TiO₂ parallelepipeds. It can then be concluded that the present films consist of single-crystalline rutile TiO₂ rectangular parallelepipeds that have grown in the [001] direction. X-ray photoelectron spectroscopy (XPS) for the films revealed that they were almost free from sodium or chloride ion contamination (see Supporting Information).

TiO₂ (generally in anatase) films have been fabricated so far using aqueous TiCl₃ via the anodic oxidative hydrolysis.[13−16] The chemical reactions were invoked as follows:[13,15]

$$Ti^{3+} + H_2O \rightarrow TiOH^{2+} + H^+ \tag{1}$$

$$TiOH^{2+} \rightarrow e^- + Ti(IV) \text{ oxo species} \rightarrow TiO_2 \tag{2}$$
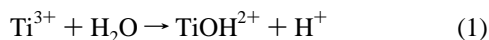
The Ti(IV) oxo species is assumed to be an intermediate between TiO²⁺ and TiO₂, consisting of partly dehydrated polymeric Ti(IV) hydroxide.[13,17] TiOH²⁺ can also be produced in the present aqueous

TiCl₃ solutions due to hydrolysis. However, the oxidation of TiOH²⁺ to the Ti(IV) oxo species does not follow the reaction 2 because our method is free from electrochemical processes. We examined the film deposition behavior in two other solutions that were saturated with oxygen and nitrogen. The film deposition was found to be promoted in the oxygen-saturated solution, while the nitrogen-saturated solution did not lead to the formation of the rutile film (see Supporting Information). The oxidation process can then be a reaction with dissolved oxygen;

$$TiOH^{2+} + O_2 \rightarrow Ti(IV) \text{ oxo species} + O_2^- \rightarrow TiO_2 \tag{3}$$

The film deposition in the solutions follows heterogeneous nucleation driven by lower degrees of supersaturation.[18] In the present case, a low degree of supersaturation with the Ti(IV) oxo species can be achieved by the slow oxidation process consuming dissolved oxygen. We confirmed that films could not be deposited when using aqueous TiCl₄ solutions under the same experimental conditions. Furthermore, the aqueous TiCl₃ solution without the NaCl addition led apparently to higher degrees of supersaturation, resulting in homogeneous nucleation of TiO₂ as precipitated powders. The role of NaCl (as Cl⁻) can then be two-fold; one is retarding formation of TiO₂ by changing the composition or coordination structure of the growing unit,[8] and the other is influencing the morphology through adsorption of Cl⁻ onto the (110) plane of rutile TiO₂.[19] Growth of TiO₂ can then be suppressed and accelerated in the [110] and the [001] direction, respectively.

Supporting Information Available: A low-magnification FE-SEM image and XPS spectra of the film, FE-SEM images of the films deposited in the oxygen- or nitrogen-saturated solutions, and experimental procedures and results for evaluation of the photocatalytic activity of the rutile film. This material is available free of charge via the Internet at http://pubs.acs.org.

References

(1) Kumar, K.-N. P.; Keizer, K.; Burggraaf, A. J. *J. Mater. Sci. Lett.* **1994**, *13*, 59−61.
(2) Jia, J. G.; Ohno, T.; Matsumura, M. *Chem. Lett.* **2000**, 908−909.
(3) Sun, J.; Gao, L.; Zhang, Q. *J. Am. Ceram. Soc.* **2003**, *86*, 1677−1682.
(4) Park, N. G.; van de Lagemaat, J.; Frank, A. J. *J. Phys. Chem. B* **2000**, *104*, 8989−8994.
(5) Kim, K. J.; Benksten, K. D.; van de Lagemaat, J.; Frank, A. J. *Chem. Mater.* **2002**, *14*, 1042−1047.
(6) Terabe, K.; Kato, K.; Miyazaki, H.; Yamaguchi, S.; Imai, A.; Iguchi, Y. *J. Mater. Sci.* **1994**, *29*, 1617−1622.
(7) Slunecko, J.; Kosec, M.; Holc, J.; Drazic, G. *J. Am. Ceram. Soc.* **1998**, *81*, 1121−1124.
(8) Cheng, H.; Ma, J.; Zhao, Z.; Qi, L. *Chem. Mater.* **1995**, *7*, 663−671.
(9) Kim, S. J.; Park, S. D.; Jeong, Y. H. *J. Am. Ceram. Soc.* **1999**, *82*, 927−932.
(10) Komarneni, S.; Rajha, R. K.; Katsuki, H. *Mater. Chem. Phys.* **1999**, *61*, 50−54.
(11) Yamabi, S.; Imai, H. *Chem. Lett.* **2001**, *30*, 220−221.
(12) Yamabi, S.; Imai, H. *Chem. Mater.* **2002**, *14*, 609−614.
(13) Kavan, L.; O'Regan, B.; Kay, A.; Grätzel, M. *J. Electroanal. Chem.* **1993**, *346*, 291−307.
(14) Kim, K. J.; Kim, G. S.; Hong, J. S.; Kang, T. S.; Kim, D. H. *Sol. Energy* **1998**, *64*, 61−66.
(15) Matsumoto, Y.; Ishikawa, Y.; Nishida, M.; Ii, S. *J. Phys. Chem. B* **2000**, *104*, 4204−4209.
(16) Lei, Y.; Zhang, L. D.; Fan, J. C. *Chem. Phys. Lett.* **2001**, *338*, 231−236.
(17) Rotzinger, F. P.; Grätzel, M. *Inorg. Chem.* **1987**, *26*, 3704−3708.
(18) Niesen, T. P.; De Guire, M. R. *J. Electroceram.* **2001**, *6*, 169.
(19) Huang, Q.; Gao, L. *Chem. Lett.* **2003**, *32*, 638−639.

JA048820P